# Effects of Shoulder-belt Slip on the Kinetics and Kinematics of the THOR

Suzanne Tylko, Kathy Tang, François Giguère, Alain Bussières

**Abstract** In a large majority of frontal offset crash tests, the shoulder belt for the driver seat is observed to slip into the gap between the neck and shoulder of the THOR anthropometric test device (ATD) and remain entrapped. The purpose of the study is to investigate and quantify the effect of shoulder-belt slip with entrapment on the kinetic and kinematic responses of the THOR in near-side oblique and full frontal crash test configurations.

The THOR ATD was installed, as per the THOR positioning procedure, in the driver seat of vehicles undergoing moving car-to-moving car frontal 40% offset crash tests (n=45) and full frontal rigid barrier tests (n=13). Three additional tests were conducted on a purpose-built sled buck at 33 km/h to corroborate in-vehicle findings and quantify forward excursion. Belt slip and entrapment were confirmed with high speed video images. Belt entrapment was associated with greater peak fore-aft and lateral shear at the lower neck, reduced fore-aft loads at the inboard and outboard left clavicle, and reduced fore-aft chest deflections in the upper left and lower right quadrants. Overlay of sled videos shows an increased head excursion. Findings may have implications for oblique test configurations used in New Car Assessment Programs.

**Keywords** Driver location, Nearside, Frontal offset crash test, Neck gap, THOR shoulder.

## I. INTRODUCTION

The Crashworthiness Research programs are mandated to provide Transport Canada with the necessary scientific foundation for the development of new motor vehicle safety standards and the introduction of new anthropometric test devices (ATDs) into regulation. A large portion of the program includes the crashworthiness evaluation of new and emerging electric and hybrid electric vehicle technologies, as well as light-weighted vehicles. The frontal offset vehicle-to-vehicle test configuration is utilised because it is a representative collision scenario in the field and is well suited for paired comparisons of crash protection.

During the course of the research program, belt slip with entrapment (Fig. 1) has been consistently observed for the THOR placed in the driver position. Early in the event the shoulder belt slides in-board, slides over the lip of the jacket collar and drops into the gap located between the neck and jacket of the left THOR shoulder. Belt entrapment in the THOR has been reported in the past, although studies of its effects on the THOR response, to our knowledge, are limited and were conducted with earlier build levels of the THOR [1-3]. Belt paths on post mortem human subjects (PMHS) have been observed to differ from those on the THOR SD-1 in frontal sled tests [4]. In angled sled tests, the belt was observed to compress the soft tissue of the PMHS; however, belt entrapment on the THOR was not reported [2]. These differences in belt path may lead to variations between THOR and PMHS responses. This paper presents an analysis of the frontal 40% offset and rigid barrier crash tests undertaken to examine the effects of shoulder-belt slip and entrapment on the kinetic and kinematic responses of the THOR.

Suzanne Tylko is Chief of Crashworthiness Research at the Centre for Innovation for Transport Canada (Suzanne.tylko<at>tc.gc.ca); Kathy Tang, François Giguère, and Alain Bussières form part of the crash data analysis team at PMG Technologies, Québec, Canada.

(A) Slip with entrapment (B) No-Slip

Fig. 1. Photos of shoulder-belt position in (A) slip and (B) no-slip conditions.

## II. METHODS

### *Crash Tests*

The sample included frontal crash tests where the view of the shoulder-belt movement on the THOR driver was not obstructed. This included frontal offset moving car-to-moving car (n=45) and full frontal rigid barrier (n=13) tests all conducted at 48 km/h.

Frontal offset test vehicles were aligned to obtain a 40% overlap on the driver side (Fig. A1, Appendix A). Overlap was calculated as 40% of the width of the narrower vehicle. Each test vehicle was propelled by a Messring closed loop electrically powered system to a velocity of 48 km/h ± 0.5 km/h and guided by a Messring MicroTrack rail (MESSRING Systembau GmbH, Krailling, Germany). Rigid barrier test vehicles were propelled into the rigid barrier at 48 km/h ± 0.5 km/h using the same propulsion and guidance system. Uni-axial accelerometers (Endevco 7264B, Meggitt, Irvine, California, USA or MSI 64B, TE Connectivity, Schaffhausen, Switzerland) were mounted on a triaxial block and installed at the approximate centre of gravity of each vehicle. Un-axial accelerometers were placed at the base of each B-pillar.

The THOR dummy was positioned as per the NHTSA THOR-50$^{th}$ percentile Male Metric Driver Dummy Seating & Positioning Procedures [5]. Measurements were recorded using a FaroArm Platinum Arm 3D metrology system (FARO, Lake Mary, Florida, USA) and onboard tilt sensors (ARS PRO-8K, DTS, Seal Beach, California, USA) located in the head and chest.

The D-ring was adjusted to position the seatbelt in the centre of the shoulder. In some tests the belt was placed further outboard to see if this might reduce slippage of the belt into the gap. Measurements of the seat-belt placement were estimated from pre-test photos using the Fiji [6] Measure tool. The distance from the outboard edge of the THOR jacket shoulder seam to the inboard edge of the shoulder belt (A) was divided by the width of the THOR jacket at the shoulder seam (Fig. 2. line B). This ratio was used to quantify the initial position of the shoulder belt relative to the neck, where a larger value suggests that the initial seat belt position is closer to the THOR neck.

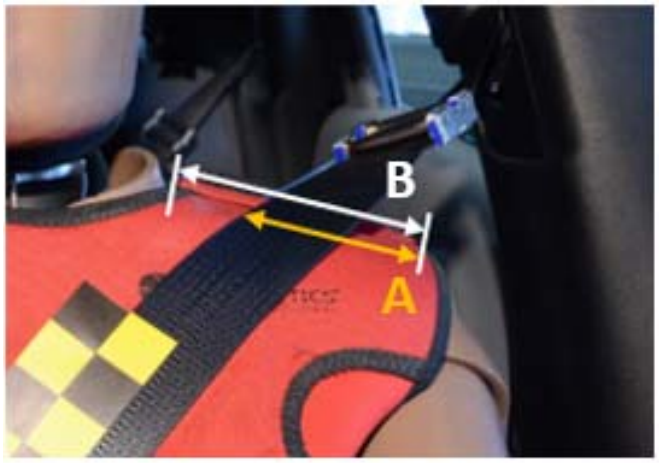


Fig. 2. Position of the shoulder belt.

***Sled Tests***

In addition to the vehicle tests, three sled tests were run with the THOR. The sled buck featured the driver seat of a 2017 Mazda Mazda3 rigidly mounted on a steel plate and installed on a MESSRING HYDROBRAKE decelerative sled. The mounting plate was oriented at an angle of 10$^{o}$ (clockwise) to replicate – to the extent possible – the lateral forces and displacements observed in the frontal offset tests. The geometry of the seatbelt anchors replicated that of the vehicle. However, the D-ring was attached to a mounting plate with several threaded holes spaced vertically at 25.4 mm intervals to allow for adjustments. Since there was no airbag or front structure to decelerate the ATD, the sled pulse as shown in Fig. 3, was limited to a delta V of 33 km/h and 20 g peak to reduce the risk of damage to the THOR. The pretensioner was fired at 0 msec and replaced, along with the seatbelt assembly, after each test.

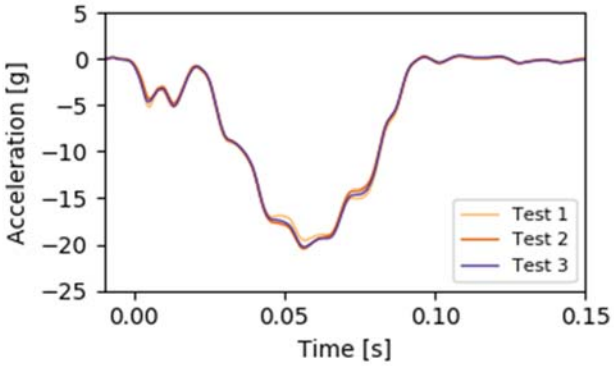


Fig. 3. Sled Pulse

The THOR dummy was placed in the seat with the legs extended and feet resting on the heels. The seat back was set to 25 $^{o}$ to replicate the in-vehicle orientation. The dummy head and thorax angles as measured by the on-board tilt sensors were within the range prescribed by the NHTSA procedures. The arms were extended forward with hands in contact with the seat. The D-ring position was modified between tests to observe the effect of shoulder-belt position on belt slippage. The three tests were run with the D-ring in the lowest (Test 1), second-lowest (Test 2), and fifth-lowest (Test 3) notches. The ratios corresponding to the initial belt positions were 0.66, 0.74, and 0.82, respectively. The placement of the belt in each test is shown in Fig. 4.

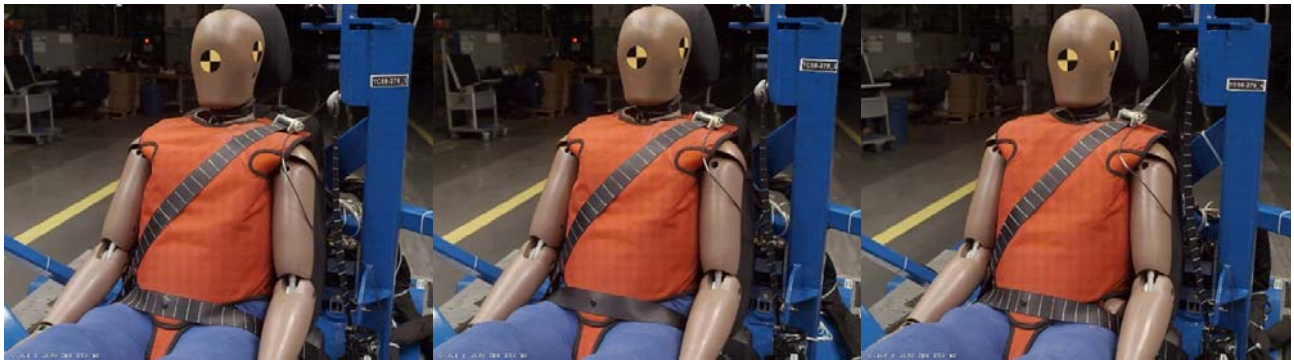

(A) Position 1 distal from the neck (B) Position mid-way (C) Position 5 proximal to the neck

Fig. 5. Photos of seatbelt placement and D-ring positions for the sled tests.

***Instrumentation and Video Imaging***

The ATD was the THOR-50M Standard SBL-B (Humanetics, Farmington Hills, Michigan, USA). A complete list of instrumentation is presented in Appendix A (Table AI). Data were recorded at 10 kHz and filtering was performed in accordance with SAE J211. High-speed videos recorded at 1000 frames/second were obtained and included a rear shoulder view (Fig. 6(A)), an oblique view centered behind the two front row seats (Fig. 7(B)), and a lateral view from the front passenger window (Fig. 8(C)).

(A) Rear shoulder view (B) Oblique view (C) Lateral view

Fig. 9. Camera views of THOR ATD in driver position.

***Data Analysis***

Videos were reviewed and each test was classified in one of three categories for further analysis. The categories were as follows:

1. Slip: the belt slips off the shoulder into the neck gap and becomes entrapped (Fig. 1(A));
2. No-slip: the belt is retained on the shoulder (Fig. 1(B));
3. Slide: the belt moves along the shoulder but drops into the gap at/ or after contact with the airbag.

The subsets of frontal offset, rigid barrier, and sled tests were each analyzed separately. Due to the infrequent occurrence of belt entrapment in rigid barrier tests, statistical and population-level analysis focused on data obtained from offset tests. Since shoulder-belt trajectories of tests in the 'slide' category were quite variable, we focused on comparisons between only the 'no-slip' and 'slip' categories, where differences were more consistently seen and clearly distinguishable.

Since all sample sizes used were less than 30, a normal approximation could not be applied. Therefore, the nonparametric two-sample Anderson-Darling test [7] was used to test for differences in empirical distributions of data obtained from tests with and without belt entrapment. Significance levels were calculated using the scipy.stats.anderson_ksamp implementation available from the Python library SciPy [8]. The advantages of the Anderson-Darling test are that it does not assume underlying distributions and it requires few assumptions about the data. However, since it is sensitive to differences in the tails of distributions, a second test must be used to confirm whether average values are significantly different. Therefore, the sample means were compared using the two-sample bootstrap hypothesis test.

Bootstrapping, a method by which sample observations are re-sampled with replacement [9], can be used to estimate confidence intervals and construct hypothesis tests for an estimator. Bootstrap distributions of the mean values of response peaks for cases where belt entrapment occurred were compared to those where it did not. Bootstrap distributions were tested against the null hypothesis that the observations obtained from tests with and without entrapment were sampled from the same distribution. Bootstrap p-values were estimated using Algorithm 16.1 of [10]. Since the p-values obtained using this method were either well over or well under 0.05, fluctuations in the value due to bootstrap sampling respectively stayed above and below the 5% significance level, giving confidence to the values reported.

## III. RESULTS

Three types of belt displacement were observed in the videos. In the 'no-slip' category, the shoulder belt remained on the shoulder throughout forward excursion. In the 'slide' category, the belt was observed to slide towards the neck and became entrapped in the gap as the dummy approached peak excursion or airbag contact, while the slip condition was characterised by obvious slippage and entrapment in the gap at the onset of forward excursion.

The 'slip' condition was observed much more frequently in frontal offset tests than in frontal rigid barrier tests. As shown in Table I, 60% of frontal offset tests were observed to have belt slippage with belt entrapment compared to 8% of rigid barrier tests. The belt remained on the shoulder of the THOR in only 27% of offset tests compared to 84% of rigid barrier tests. The slide category was observed in only six offset tests and one rigid barrier test.

TABLE I
DISTRIBUTION OF BELT RESPONSES OBSERVED IN TESTS

| Category | Frontal Offset | Rigid Barrier | Sled Buck | Total |
|---|---|---|---|---|
| No-Slip | 12 (0.27) | 11 (0.84) | 1 | 24 |
| Slide | 6 (0.13) | 1 (0.08) | 1 | 8 |
| Slip | 27 (0.60) | 1 (0.08) | 1 | 29 |
| Total | 45 | 13 | 3 | 58 |

***Offset Tests***

The most notable differences in responses between tests with and without belt entrapment (i.e. those with the lowest p-values) occurred at the lower neck and upper left quadrant of the chest. In frontal offset tests with belt entrapment, the magnitudes of the mean peak fore-aft and lateral shear forces in the lower neck were 1320 N and 1000 N greater, respectively than in tests where the belt remained on the shoulder (Table II). The differences in means and empirical distributions of the peak values are statistically significant by the bootstrap hypothesis test and the two-sample Anderson-Darling test, respectively. Comparisons of both the fore-aft and lateral shear loads yield p=0 by the bootstrap hypothesis test because there is no overlap in the ranges of peak values between the two different conditions ('slip' vs 'no-slip'). The mean time to peak of lateral neck force was delayed by 15 msec with belt entrapment, a difference that was significant at the 5% level by both the bootstrap hypothesis test and Anderson-Darling test. On the other hand, the 6 msec delay observed in the time to peak of the fore-aft load was significant by the Anderson-Darling test, but not by the bootstrap hypothesis test.

TABLE II
COMPARISON OF FORE-AFT AND LATERAL LOWER NECK FORCES IN FRONTAL OFFSET TESTS

| Direction [units] | Mean ± std | | Difference | Bootstrap p-value | Anderson-Darling p-value |
|---|---|---|---|---|---|
| | No-Slip (n=12) | Slip (n=27) | | | |
| Fore-Aft Peak [N] | 110 ± 90 | 1430 ± 350 | 1320 | 0 | <0.001 |
| Lateral Peak [N] | -280 ± 190 | 1280 ± 300 | 1000 | 0 | <0.001 |
| Fore-Aft Time to Peak [msec] | 88 ± 29 | 94 ± 6 | 6 | 0.16 | 0.013 |
| Lateral Time to Peak [msec] | 85 ± 23 | 100 ± 6 | 15 | 0.002 | 0.002 |

The upper left quadrant and lower right quadrant chest deflections (in X) were reduced by 6 mm and 7 mm, respectively, for tests with belt entrapment (Table III). The differences between the mean values and empirical distributions for the peak displacement values at both quadrants of the chest were statistically significant. Despite noticeable differences in the magnitude of peak displacement, neither quadrant showed significant difference in the time to peak. The Principal Component (PC) score as calculated with the Diadem software (National Instrument Corporation, Austin, TX) was not significantly different in tests with and without slippage.

Results of other responses resulting from the slip and no-slip condition are summarised in Table IV. Effects of belt entrapment included: reduced left clavicle load; higher peak lateral accelerations of the upper spine and chest; increased angular velocity of the thorax (rotation about z); and increased axial loads in the left femur. These differences were all statistically significant at the 5% level.

TABLE III
COMPARISON OF CHEST DISPLACEMENTS IN FRONTAL OFFSET TESTS

| Quadrant [units] | Mean ± std | | Difference | Bootstrap p-value | Anderson-Darling p-value | Sample Size (no-slip/slip) |
|---|---|---|---|---|---|---|
| | No-Slip | Slip | | | | |
| Upper Left Peak Dx [mm] | -20 ± 5 | -14 ± 4 | 6 | 0.001 | 0.001 | 12/27 |
| Lower Right Peak Dx [mm] | -31 ± 6 | -24 ± 6 | 7 | 0.001 | 0.006 | 12/26 |
| Upper Left Time to Peak [msec] | 74 ± 11 | 73 ± 13 | 1 | 0.36 | 0.69 | 12/27 |
| Lower Right Time to Peak [msec] | 73 ± 16 | 65 ± 16 | 8 | 0.076 | 0.51 | 12/26 |
| Chest Deflection PC Score | 5.6 ± 0.7 | 5.6 ± 0.8 | 0 | 0.39 | 0.78 | 12/20 |

TABLE IV
SUMMARY OF THOR RESPONSES FROM THE SLIP AND NO-SLIP CONDITION IN FRONTAL OFFSET TESTS

| Channel [units] | Mean ± std | | Bootstrap p-value | Anderson-Darling p-value | Sample Size (No-Slip/Slip) |
|---|---|---|---|---|---|
| | No-Slip | Slip | | | |
| Outer Left Clavicle Load X [N] | -385 ± 119 | -203 ± 141 | 0.001 | 0.001 | 12/26 |
| Inner Left Clavicle Load X [N] | -562 ± 154 | -419 ± 193 | 0.018 | 0.018 | 12/24 |
| Upper Spine Acceleration X [g] | -39.0 ± 4.1 | -47.7 ± 10.6 | 0.003 | 0.006 | 12/27 |
| Upper Spine Acceleration Y [g] | 11.5 ± 4.1 | 17.9 ± 9.1 | 0.010 | 0.013 | 12/27 |
| Chest Acceleration Y [g] | 15.8 ± 4.7 | 21.1 ± 5.2 | 0.002 | 0.006 | 12/26 |
| Thoracic Spine Ang. Velocity Z [deg/s] | 211 ± 127 | 446 ± 186 | <0.001 | <0.001 | 12/27 |
| Left Femur Force Z [N] | -2410 ± 2410 | -3560 ± 1830 | 0.002 | 0.009 | 12/27 |

The time history plots presented in Fig. 10 compare the mean and 90$^{th}$ percentile corridors for lower neck shear and two chest quadrants in the slip and no-slip condition for offset tests. The heavier line and darker shading represent the slip condition while the lighter line and lighter shading represent the no-slip condition. The average peak fore-aft shear (Fig. 11(A)) for the slip condition is 1320 N greater than the non-slip condition. The average peak lateral shear (Fig. 12(B)) is 1000 N greater for the slip condition. The average peak upper left (Fig. 13(C)) and lower right (Fig. 14(D)) chest displacements were reduced by 6 mm and 7 mm respectively, in the slip condition.

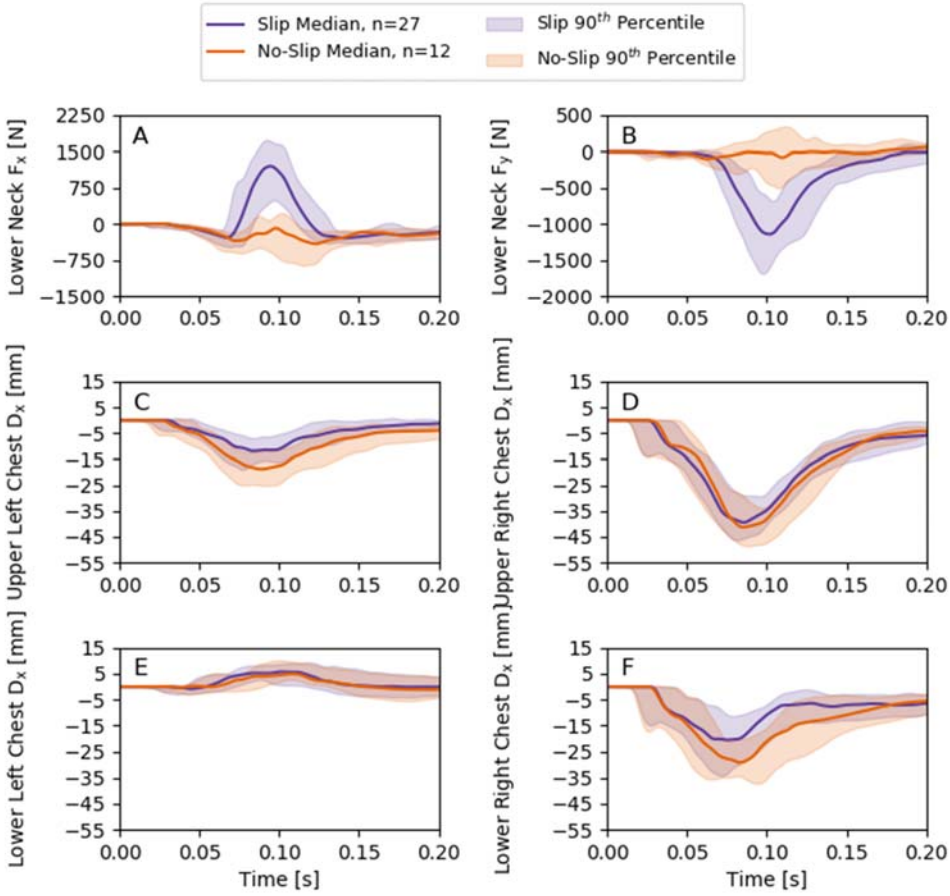


Fig. 15. Comparison of lower neck loads (fore-aft $F_X$, lateral $F_Y$) and chest displacements in X ($D_X$) in frontal offset tests with and without belt entrapment.

To estimate the time at which the THOR response in 'slip' and 'no-slip' conditions started to diverge, we combined the sample of offset tests with 'slip' and 'no-slip' outcomes and found the time at which the variance of this combined sample started to exceed typical fluctuations present within the individual subsamples. To do so, the time-varying standard deviation of the combined sample was compared to those of each subsample. The initial time at which the standard deviation of the combined sample exceeded that of both subsamples for at least 5 msec was considered to be an upper bound for the time of deviation. An initial time of deviation could not be identified for all channels. However, for the responses where differences could be identified, all of the changes in response started to occur before 80 msec (Table V). Differences in left clavicle loads started to occur at 44 and 47 Msec. These differences were followed by differences in chest displacement, which occurred at 61 msec. Finally, differences in the thoracic spine angular velocity and in lower neck loads occurred at 70-80 msec.

TABLE V

TIME OF INITIAL DEVIATION BETWEEN 'SLIP' AND 'NO-SLIP' RESPONSES IN FRONTAL OFFSET TESTS

| **Channel** | **Time of Initial Deviation [s]** |
|---|---|
| Outer Left Clavicle Load X | 0.0444 |
| Inner Left Clavicle Load X | 0.0473 |
| Upper Left Chest Displacement X | 0.0611 |
| Lower Right Chest Displacement X | 0.0623 |
| Lower Neck Force Y | 0.0724 |
| Thoracic Spine Angular Velocity Z | 0.0730 |
| Lower Neck Force X | 0.0754 |

Initial belt position was found to influence the likelihood of belt entrapment. The pre-test belt position ratio as defined by the distance of in-board belt edge divided by width of jacket at the shoulder seam ranged from 0.5 to 0.95. The distributions of 'slip' and 'no-slip' tests as a function of the pre-test belt position ratio are shown in Fig. 16(A). Initial belt positions closer to the neck result in a slip far more frequently than a 'no-slip', and likewise, positions further away from the neck are more likely to fall under 'no-slip'. However, the relationship between pre-test ratio and time to slip shown in Fig. 17(B) appears to be weak ($R^2 = 0.4$). Figure 18(C) shows a clear distinction in the peak lower neck lateral shear for the slip and no-slip cases. For slip cases, peak lower neck shear loads tend to increase as the pre-test position approaches the neck. Fig. 19(D) presents the timing of these peak loads and suggests an association between time to peak and magnitude of the lower neck shear.

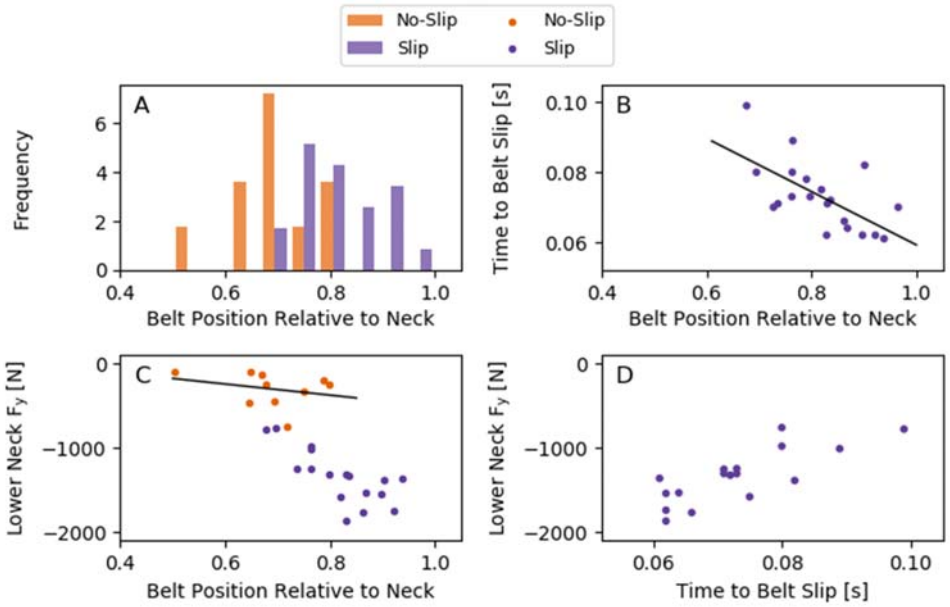


Fig. 20. Relationship between belt position, time to belt slip, and THOR response at the lower neck.

***Barrier Tests***

There were not enough slip cases in the rigid barrier test sample (n=1) to report on ensemble statistics. There was, however, a matched pair of test vehicles where a 'slip' was observed in one but not the other. The results, summarised in Table VI, are consistent with those reported for frontal offset tests. The initial shoulder belt position was close to the THOR neck in the test with belt entrapment (0.90 with entrapment vs. 0.69 without entrapment). Neck shear was more elevated for the slip case, as were the femur loads. A comparison with the population of responses obtained from 'no-slip' conditions is summarised in Table AII.

TABLE VI
COMPARISON OF THOR RESPONSES IN PAIRED RIGID BARRIER IMPACT

| **Channel [units]** | **No-slip** | **Slip** |
|---|---|---|
| Fore-Aft Neck Force [N] | 141 | 798 |
| Lateral Neck Force [N] | -351 | -1054 |
| Upper Left Chest Displacement [mm] | -18.6 | -12.3 |
| Lower Right Chest Displacement [mm] | -28.4 | -23.6 |
| Outer Left Clavicle Load [N] | -392 | -163 |
| Inner Left Clavicle Load [N] | -795 | -464 |
| Upper Spine Acceleration X [g] | -39.6 | -46.4 |
| Upper Spine Acceleration Y [g] | 3.89 | 11.9 |
| Chest Acceleration Y [g] | 8.57 | 14.0 |
| Thoracic Spine Angular Velocity Z [deg/s] | 155 | 396 |
| Left Femur Force Z [N] | -3130 | -3760 |
| PC Score | 5.4 | 5.4 |

***Sled Tests***

To validate the effects observed with belt entrapment in frontal offset and rigid barrier tests, three sled tests were performed to reproduce the 'no-slip', 'slide', and 'slip' conditions. Consistent with the in-vehicle tests, the 'slip' condition resulted in higher fore-aft (Fig. 21(A)) and lateral (Fig. 22(B)) loads at the lower neck; lower chest displacements in the upper left (Fig. 23(C)) and lower right (Fig. 24(D)) quadrants; and lower loads on the inner and outer left clavicle when compared to the 'no-slip' condition. The peak magnitudes of the 'slide' response fell between those observed with 'slip' and 'no-slip'. As with the offset and rigid barrier tests, PC scores obtained from the 'slip' and 'no-slip' tests were very similar (difference of 0.03). Differences in the responses of the upper spine (fore-aft and lateral) and lateral chest accelerations that had been observed in the vehicle tests were not reproduced on the sled. Since there was no forward structure to load the knees, femur loads were not compared.

The repeatable test environment of the sled buck allowed for a comparison of head excursions. Figure 25 presents overlays of two freeze frame images captured at peak excursion for the slip and no-slip conditions. The excursion of the slip response identified by line B is greater than the no-slip response identified by line A.

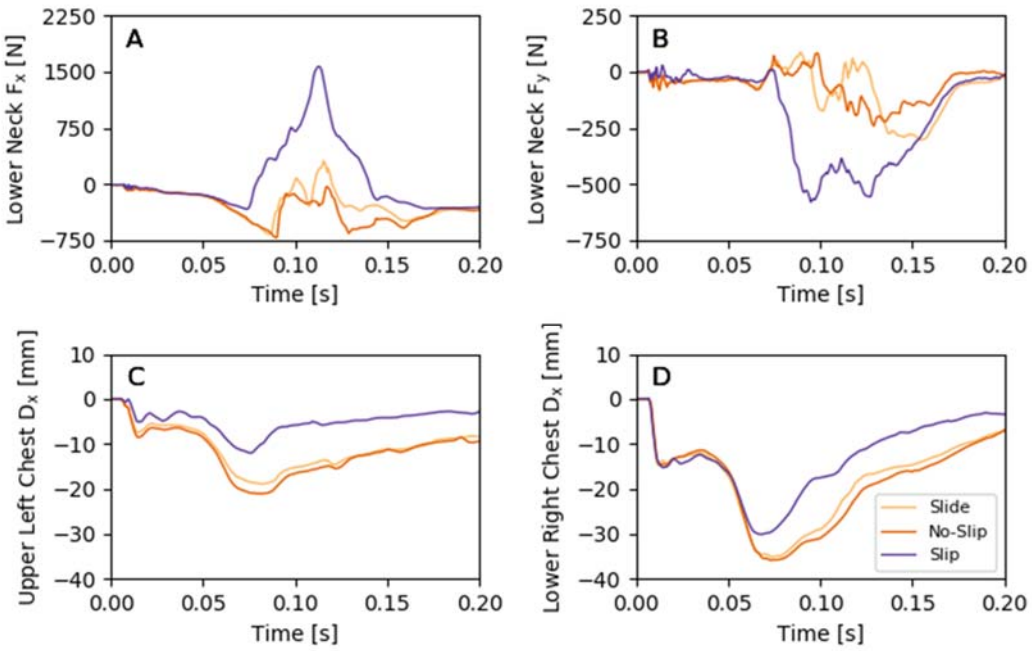


Fig. 26. Time history of lower neck load and chest displacement in sled tests reproducing the No-Slip (dark orange), 'Slide' (orange), and Slip (purple) responses.

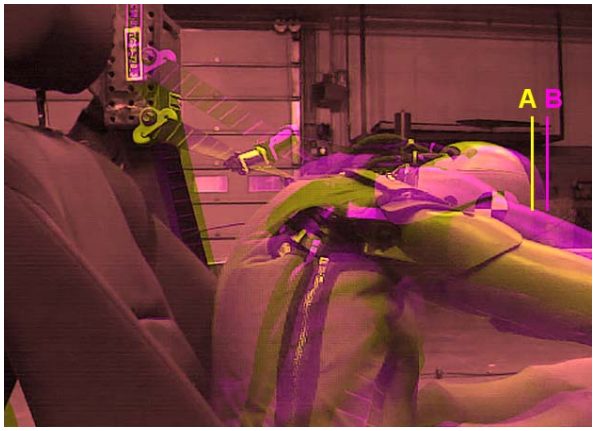


Fig. 27. Excursion observed for No-Slip (A) and Slip (B) conditions in sled tests.

## IV. DISCUSSION

The purpose of this study was to characterise the effect of shoulder-belt slip and entrapment on the kinetic and kinematic responses of the THOR in near side frontal offset and full frontal crash test configurations. In frontal offset crash tests, belt entrapment was associated with greater peak fore-aft and lateral lower neck shear, reduced fore-aft loads at the inner and outer left clavicle, and reduced chest deflections (in X) in the upper left and lower right quadrants. In vehicle tests, peak lateral accelerations at T1, in combination with elevated peak angular velocity of the thoracic spine suggest that belt entrapment was associated with increased outboard motion and clockwise rotation of the torso. In 2006, Törnvall, et al. [1] conducted 30° near-side sled tests and reported that the head of the THOR Alpha moved further forward and that the shoulders tended to move slightly more sideways and downwards compared to the PMHS. There was no mention of belt slip or entrapment for the near side configuration. In a follow-up study with the THOR NT and THOR SD-$1_{NT}$, Törnvall, et al. [2] described belt slip along the clavicle and into the inferior region of the neck, reducing loads to the shoulder. While they reported increased lateral motion of the THOR, they did not specifically attribute this to belt entrapment, but rather to more general shoulder design characteristics. Belt slip along the clavicle and into the soft tissues of the neck was also observed with the PMHS, however the authors did not elaborate on how

this compared to the THOR.

Femur loads were found to be higher for the slip cases in both the offset and barrier tests. This may be indicative of increased forward excursion. However, since measurements of distance from the knees to the point of contact on the lower instrument panel were not available, it was not possible to quantify the effects of increased femur loads independently of pre-test proximity. The paired Mazda 3 barrier tests in which the THOR positions were matched did permit a direct comparison to be carried out. In this comparison the slip condition resulted in a 600 N increase in femur axial loads compared to the no-slip. This suggests that for this vehicle pair, the belt slippage was associated with a greater forward excursion of the dummy. Three sled tests were conducted to better visualise the motion of the THOR as a function of slip, no-slip and the intermediate slide condition and to verify the trends observed during in-vehicle crash tests. Even though the sled pulse was less severe than the vehicle pulse, overlays of videos confirm that head excursion was greater for the slip condition. The increase in lower neck shear and lower chest displacements associated with belt slippage were replicated in the sled tests, confirming that the response caused by belt slip can be replicated. The increased shear loading to the lower neck associated with the slip condition in the vehicle and sled configurations may be indicative of a displaced load path.

***Seat-belt Geometry and Crash Configuration***

By estimating the times at which the responses associated with and without belt entrapment started to deviate from each other, we found that changes in clavicle load, chest displacement, and lower neck loads occurred before the belt became completely entrapped. Notably, changes in the geometry of the shoulder belt were detected by the clavicle load cell and the chest deflection sensors before the belt had completely penetrated the gap between the shoulder and the neck. Monitoring of these responses could serve as a predictor of belt slippage in the absence of visual confirmation.

Comparison of belt geometries showed that belt entrapment occurred more frequently and more quickly when the initial position of the shoulder belt was close to the neck and when there was an offset component to the crash. Eggers, et al. [3] showed that manipulation of belt geometry by altering the D-ring height leads to differences in chest deflection, but there was no mention of belt entrapment. As the belt is displaced inboard, it moves away from the point of measurement in the upper left quadrant, and that deflection is reduced. What is less obvious is the relationship between the belt geometry, the principal direction of force, and the frequency of entrapment.

Shaw, et al. [4] compared the thoracic response of the THOR-NT and THOR SD-1 to PMHS in frontal sled tests. They found that the SD-1 shoulder and jacket modifications displaced the shoulder-belt path and that it was the belt geometry rather than the shoulder design (shielding) that influenced the thoracic deflection response. The belt geometry was also found to affect peak fore-aft accelerations at the T1 position. They reported that movement of the belt was towards the neck on the ATDs, but on the PMHS was towards the shoulder. In a more recent study, Shaw, et al. [11] confirmed the relationship between deflection response and distance from the point of measurement in the THOR SD-3, but did not report on belt placement or belt movement.

Extensive biofidelity results recently published by Parent, et al. [12] indicate that the THOR has good biofidelity. While this is promising, the sled tests included in the biofidelity study did not include near side oblique sled tests. Given that belt entrapment causes such a large vertical displacement of the belt relative to the shoulder and appears to transfer belt loads to the lower neck, further biofidelity studies comparing the latest THOR build level to PMHS should be carried out. Mathematical models, such as those developed for the THORAX-FP7 [13] may be beneficial. Finally, the difference observed with belt entrapment did not appear to directly affect injury metrics currently referenced by consumer test programs for oblique or small overlap impacts test protocols. However, given the complexity of designing safety countermeasures that limit contact with the interior structures of the vehicle [14]--[15], accurate representation of the head and upper body trajectories in the THOR, are especially important.

The advantages of in-vehicle testing are offset by the absence of excursion measures and the challenge of controlling for the effect of vehicle design variability. This analysis focused only on the characterisation of peak magnitude and timing seen in the responses of the THOR. The low frequency of occurrence of belt slip in the rigid barrier configuration restricted the comparison of slip to no-slip conditions in full frontal barrier conditions.

## V. CONCLUSIONS

- Belt slip and entrapment were more likely to occur in near-side frontal offset tests and when the initial position of the belt was close to the THOR neck.
- Belt slip with belt entrapment were associated with greater peak fore-aft and lateral lower neck shear and reduced fore-aft loads at the inner and outer left clavicle.
- The reduced chest deflections in the upper left and lower right quadrants were likely due to displacement of the shoulder belt away from the point of measurement.
- In vehicle tests, peak lateral accelerations at T1, in combination with elevated peak angular velocity of the thoracic spine, suggest that belt entrapment was associated with increased outboard motion and clockwise rotation of the torso.
- Belt slip and entrapment may lead to increased forward excursions as supported by increased axial loading of the femurs in the paired rigid barrier test and increased head excursion in the sled test.
- Biofidelity of the THOR in near side oblique sled tests should be evaluated.

## VI. ACKNOWLEDGEMENTS

The authors gratefully acknowledge the staff at PMG Technologies for conducting the tests, and the technical assistance of Samuel Filipe Pedroso and Pierre Villemure of the Centre for Innovation.

## VII. DISCLAIMER

This paper shall not be construed as an endorsement, warranty, or guarantee, expressed or implied, on the part of Transport Canada for any evaluated material, product, system or service described herein. Readers should not infer that Transport Canada's evaluation is for any purpose or characteristic other than as stated herein. All information in this document is for information purposes, only and is not intended to provide any specific advice. Any reliance on or use of the information contained in this document is at the user's sole risk and expense.

## VIII. REFERENCES


[1] Törnvall, F. V., Svensson, M. Y., Davidsson, J., Flogard A., Kalliaris D., Haland Y. (2005) Frontal Impact Dummy Kinematics in Oblique Frontal Collisions: Evaluation Against Post Mortem Human Subject Test Data, *Traffic Injury Prevention*, **6**(4): pp.340-350.

[2] Törnvall, F. V., Holmqvist, K., Davidsson, J., Svensson, M. Y. (2008) Evaluation of Dummy Shoulder Kinematics in Oblique Frontal Collisions. *Proceedings of IRCOBI Conference*, 2008, Bern, Switzerland.

[3] Eggers, A., Eickhoff, B., Dobberstein, J., Zellmer, H., Adolph, T. (2014) Effects of Variations in Belt Geometry, Double Pretensioning and Adaptive Load Limiting on Advanced Chest Measurements of THOR and Hybrid III. *Proceedings of IRCOBI Conference*, 2014, Berlin, Germany.

[4] Shaw, G., Parent, D., Purtsezov, S., Lessley, D., Crandall, J. (2010) Torso Deformation in Frontal Sled Tests: Comparison Between THOR NT, THOR NT with the Chalmers SD-1 Shoulder, and PMHS. *Proceedings of IRCOBI Conference*, 2010, Hanover, Germany.

[5] NHTSA. (2015) "THOR Driver Seating Procedure – Draft 7-22-2015". Internet: [https://www.nhtsa.gov/document/thor-driver-seating-procedure-draftjuly-22-2015.pdf], 2015-22-07 [2018-03-29]

[6] Schindelin, J., *et al*. (2012) Fiji: an open-source platform for biological-image analysis. *Nature Methods*, **9**: pp.676-682.

[7] Scholz, F. W., Stephens, M. A. (1987) K-Sample Anderson-Darling Tests. *Journal of the American Statistical Association*, **82**(399): pp.918-924.

[8] Jones, E., *et al.* (2001) "SciPy: Open Source Scientific Tools for Python". Internet: [http://www.scipy.org], 2001- [2018-03-27].

[9] Belsley, D. A., Kontoghiorghes, E. J. (2009) Handbook of Computational Econometrics, p. 172, *Wiley*, Chichester, United Kingdom.

[10] Efron, B., Tibshirani, R. (1994) An Introduction to the Bootstrap, p. 221, *Chapman & Hall*, New York, United States.

[11] Shaw, G., Lessley, D., Ash, J., Crandall, J. (2013) Response Comparison for the Hybrid III, THOR Mod Kit with SD-3 Shoulder, and PMHS in a Simulated Frontal Crash. *23rd International Technical Conference on the Enhanced Safety of Vehicles*, 2013, Seoul, Korea.

[12] Parent, D., Craig, M., Moorhouse, K. (2017) Biofidelity Evaluation of the THOR and Hybrid III 50th Percentile Male Frontal Impact Anthropomorphic Test Devices. *Stapp Car Crash Journal*, **61**.

[13] Lemmen, P., *et al*. (2012) Development of an Advanced Frontal Dummy Thorax Demonstrator. *Proceedings of IRCOBI Conference*, 2012, Dublin, Ireland.

[14] Rudd, R., Scarboro, M., Saunders, J. (2011) Injury Analysis of Real-World Small Overlap and Oblique Frontal Crashes. *22nd International Technical Conference on the Enhanced Safety of Vehicles*, 2011, Washington D.C., USA.

[15] Saunders, J., Parent, D., Ames, E. (2015) NHTSA Oblique Crash Test Results: Vehicle Performance and Occupant Injury Risk Assessment in Vehicles with Small Overlap Countermeasures. *24th International Technical Conference on the Enhanced Safety of Vehicles*, 2015, Gothenburg, Sweden.

## IX. APPENDIX

Fig. A1. Top view of a 40% offset configuration

TABLE AI
LIST OF THOR ATD INSTRUMENTATION

| |
|---|
| Head CG Tri-axial Accelerometer |
| Head Accelerometers (Top) |
| Head Accelerometers (Side) |
| Head Accelerometers (Rear) |
| Head CG Angular Rate Sensor |
| Head Tilt Sensor |
| Upper Neck Load Cell |
| Lower Neck Load Cell |
| Skull Spring Load Cell (Front and Rear) |
| Clavicle Load Cell SD3 (Left and Right) |
| T1 Tri-axial Accelerometer |
| Thorax Tri-axial Accelerometer |
| T12 Tri-axial Accelerometer |
| Thoracic Tilt Sensor |
| Lumbar Tilt Sensor |
| Lumbar Load Cell |
| IR-TRACC Upper Thorax (Left and Right) |
| IR-TRACC Lower Thorax (Left and Right) |
| Upper Abdomen Accelerometer |
| IR-TRACC Abdomen (Left and Right) |
| Pelvis CG Tri-axial Accelerometer |
| Pelvic Tilt Sensor |
| Iliac Load Cell (Left and Right) |
| Acetabulum Load Cell (Left and Right) |
| Femur Load Cell (Left and Right) |
| Knee Shear Displacement Potentiometer (Left and Right) |
| Upper Tibia Load Cell (Left and Right) |
| Lower Tibia Load Cell (Left and Right) |
| Tibia Accelerometer (Left and Right) |
| Achilles Load Cell (Left and Right) |
| Ankle Rotation Potentiometer (Left and Right in X, Y, and Z) |
| Foot Acceleration (Left and Right) |

TABLE AII

DIFFERENCES IN THOR RESPONSE OBSERVED WITH BELT ENTRAPMENT IN RIGID BARRIER TESTS

| **Channel [units]** | **No-Slip (mean ± std)** | **Slip (n=1)** | **Sample Size (no-slip)** |
|---|---|---|---|
| Fore-Aft Neck Force [N] | 364 ± 256 | 798 | 11 |
| Lateral Neck Force [N] | -317 ± 88 | -1054 | 11 |
| Upper Left Chest Displacement [mm] | -24 ± 5 | -12.3 | 11 |
| Lower Right Chest Displacement [mm] | -28 ± 5 | -23.6 | 11 |
| Outer Left Clavicle Load [N] | -440 ± 218 | -163 | 10 |
| Inner Left Clavicle Load [N] | -662 ± 169 | -464 | 10 |
| Upper Spine Acceleration X [g] | -44.1 ± 2.8 | -46.4 | 11 |
| Upper Spine Acceleration Y [g] | 6.56 ± 3.7 | 11.9 | 11 |
| Chest Acceleration Y [g] | 8.52 ± 3.1 | 14.0 | 11 |
| Thoracic Spine Angular Velocity Z [deg/s] | 268 ± 113 | 396 | 7 |
| Left Femur Force Z [N] | -2850 ± 1120 | -3760 | 11 |
| PC Score | 5.3 ± 0.5 | 5.4 | 3 |